Lattice Boltzmann Model for Simulation of Magnetohydrodynamics

Shiyi Chen,[a] Hudong Chen,[b] Daniel Martínez, and William Matthaeus
Bartol Research Institute, University of Delaware, Newark, Delaware 19716
(Received 25 July 1991)

A numerical method, based on a discrete Boltzmann equation, is presented for solving the equations of magnetohydrodynamics (MHD). The algorithm provides advantages similar to the cellular automaton method in that it is local and easily adapted to parallel computing environments. Because of much lower noise levels and less stringent requirements on lattice size, the method appears to be more competitive with traditional solution methods. Examples show that the model accurately reproduces both linear and nonlinear MHD phenomena.

PACS numbers: 52.30.−q, 52.65.+z

Recent interest in lattice-gas methods for solution of fluid equations and other partial differential equations has been motivated by the need for efficient techniques for examining a wide range of difficult nonlinear problems on modern parallel computers. The cellular automaton (CA) method, with purely local Boolean operations, has shown promise for hydrodynamics [1-3], MHD [4,5], and other fluid systems [6]. Another lattice-gas method, based on the lattice Boltzmann equation (LBE), has recently been developed for hydrodynamics [7,8]. In this Letter we introduce a lattice Boltzmann equation model for MHD, based on a modification of the dynamical equation for the 36-bit MHD CA model [5]. We argue that the LBE model has a number of advantages for MHD computations relative to the CA approach, and demonstrate through numerical solutions that the model accurately reproduces solutions for several fundamental MHD processes.

The LBE approach shares with CA models the efficiency of local operations, discrete structure, and ease of parallelization, but requires, relative to CAs, many fewer lattice sites and maintains a higher signal-to-noise ratio. In addition, whereas much of the computational effort in CA dynamics is involved in the evaluation of complex Boolean collision operators, the LBE approach affords additional efficiency due to flexibility in handling collision terms. There exists a different MHD LBE model proposed by Succi, Vergassola, and Benzi for two-dimensional (2D) MHD. An extension of that model to three dimensions (3D), however, is difficult [9].

In the present MHD LBE model, moments of the one-particle distribution, corresponding to mass density, momentum, and magnetic field, are shown, in the limit of long wavelength and low frequency, to satisfy the equations of incompressible MHD. This result is obtained in either 2D or 3D, at low Mach number and high β, using techniques presented in detail for the CA model. We also introduce a simple and effective single-time relaxation model for the collision operator, which has not been applied to LBE models previously as far as we are aware. This leads to spatially homogeneous and easily controllable transport coefficients. Demonstrations of the model include accurate solutions of the classical linear Hartmann flow problem and solutions of nonlinear magnetic reconnection. We develop the MHD LBE model here for 2D; the extension to 3D is straightforward.

We adopt the standard triangular lattice consisting of hexagonal cells [1], with a cell position indicated by $\mathbf{x}$. The nearest-neighboring cells are located at $\mathbf{x}+\mathbf{e}_a$; $\mathbf{e}_a=(\cos(2\pi a/6),\sin(2\pi a/6))$, $a=1,\ldots,6$. As in the MHD CA model [5], one envisions particles residing at lattice sites, each carrying a vector quantum $\mathbf{e}_a$ corresponding roughly to momentum, and also carrying an additional vector

$$\mathbf{e}_b=(\cos(2\pi b/6),\sin(2\pi b/6)),\quad b=1,\ldots,6,$$

conveniently thought of as the magnetic field quantum. In each cell there are 36 different states, each of which is labeled by $\mathbf{e}_a$ and $\mathbf{e}_b$, or just (a,b). In contrast to the CA method, here we do not follow individual particles, but deal exclusively with the particle distribution function, $f_{ab}(\mathbf{x},t)$ which is a real-valued positive function of the discrete time and space. Like the 36-bit MHD CA, the present model propagates information on the lattice using a bidirectional streaming algorithm based on a constant parameter matrix P_{ab}, where $|P_{ab}|<1$. Here, the particle distribution in state (a,b) at position $\mathbf{x}$ at time t is split into two parts. A fractional amount $1-|P_{ab}|$ propagates, at time $t+1$, to position $\mathbf{x}+\mathbf{e}_a$, while the remainder propagates to position $\mathbf{x}+\mathrm{sgn}(P_{ab})\mathbf{e}_b$. In contrast to the CA model, this operation is completely deterministic. For clarity, we let the quantity $f_{ab}(\mathbf{x},t)$ denote the particle distribution at the time of arrival at $\mathbf{x}$. Just afterwards, the particle distribution is subjected to the collision operation Ω_{ab}, which, in the LBE approach, is constructed to drive the distribution towards an (as yet unspecified) equilibrium denoted by f_{ab}^{eq}. It follows that the discrete lattice Boltzmann kinetic equation is

$$\begin{aligned} f_{ab}(\mathbf{x},t)=&(1-|P_{ab}|)[f_{ab}(\mathbf{x}-\mathbf{e}_a,t-1)+\Omega_{ab}(\mathbf{x}-\mathbf{e}_a,t-1)]\\ &+|P_{ab}|[f_{ab}(\mathbf{x}-\mathrm{sgn}(P_{ab})\mathbf{e}_b,t-1)+\Omega_{ab}(\mathbf{x}-\mathrm{sgn}(P_{ab})\mathbf{e}_b,t-1)]. \end{aligned} \tag{1}$$

Note that the collision operator $\Omega_{ab}(\mathbf{x},t)$ only depends on the particle distribution function f at the same position and time. Correspondence of the dynamics implied by (1) to continuum physics is established through the corresponding

(low-frequency, long-wavelength [2]) continuous equation

$$\frac{\partial f_{ab}(\mathbf{x},t)}{\partial t}+\mathbf{v}_{ab}\cdot\nabla(f_{ab}+\Omega_{ab})-\tfrac{1}{2}[(1-|P_{ab}|)\mathbf{e}_a\mathbf{e}_a+|P_{ab}|\mathbf{e}_b\mathbf{e}_b]:\nabla\nabla(f_{ab}+\Omega_{ab})=\Omega_{ab} \tag{2}$$

by expansion to second order in the lattice parameters. In (2) we have introduced the particle velocity $\mathbf{v}_{ab}\equiv(1-|P_{ab}|)\mathbf{e}_a+|P_{ab}|\mathbf{e}_b$, which represents the mean velocity of particles (due to bidirectional streaming along either the a or b direction) in the state (a,b). The appearance of the collision operator, Ω_{ab} on the left-hand side of (2), takes into account the random-walk propagation process.

To clarify the role of collisions in the model, let us write the distribution as $f_{ab}=f_{ab}^{\rm eq}+f'_{ab}$, where f'_{ab} is the departure from the local equilibrium, assumed here to be small. The collision operator, taken to be a function only of the local particle distribution $f=\{f_{ab},\ a,b=1,\ldots,6\}$, can be now approximated by

$$\Omega_{ab}(f)=\Omega_{ab}(f^{\rm eq})+\sum_{c,d}f'_{cd}\partial\Omega_{ab}(f^{\rm eq})/\partial f_{cd}\,.$$

If the collision operator is chosen so that $\Omega_{ab}(f^{\rm eq})=0$, then $\Omega_{ab}(f)\propto f'$. For the most general case this proportionality would involve a fourth-rank matrix that depends on the details of the particle collision operator. Here we introduce [10] the single relaxation time τ and the approximation that $\partial\Omega_{ab}(f^{\rm eq})/\partial f_{cd}=-\tau^{-1}\delta_{ac}\delta_{bd}$. This leads to an explicit and particularly simple form of the collision operator, $\Omega=\tau^{-1}(f_{ab}^{\rm eq}-f_{ab})=-f'/\tau$.

Let us introduce the macroscopic MHD variables, mass density n, fluid velocity $\mathbf{u}$, and magnetic field $\mathbf{B}$, and their relationship to the microscopic state through the definitions $n=\sum_{ab}f_{ab}$, $n\mathbf{u}=\sum_{ab}\mathbf{v}_{ab}f_{ab}$, and

$$n\mathbf{B}=\sum_{ab}[R_{ab}\mathbf{e}_a+Q_{ab}\mathbf{e}_b]f_{ab}.$$

The matrices $\mathbf{Q}$ and $\mathbf{R}$, like $\mathbf{P}$, are 6×6 circulant parameter matrices, which have been shown [5], on the basis of rotational and inversion symmetries, to contain just two independent parameters each. In particular, we denote them as $\mathbf{P}=\text{circ}[p_0,p_1,-p_1,-p_0,-p_1,p_1]$, $\mathbf{Q}=\text{circ}[q_0,q_1,q_1,q_0,q_1,q_1]$, and $\mathbf{R}=\text{circ}[r_0,r_1,-r_1,-r_0,-r_1,r_1]$ (circ means circulant matrix). To arrive at a microscopic equilibrium corresponding to MHD, it is necessary to select a collision operator that conserves locally the mass, the momentum $n\mathbf{u}$, and the magnetic intensity $n\mathbf{B}$. A pseudo-Fermi-Dirac distribution [5], Taylor expanded for small values of velocity and magnetic field, fits these requirements, and can be written as

$$f_{ab}^{\rm eq}=d+2d\left[\frac{1}{\lambda_1}\mathbf{e}_a\cdot\mathbf{u}+\frac{1}{\lambda_2}\mathbf{e}_b\cdot\mathbf{B}\right]+4d\left[\frac{1}{\lambda_1^2}Q_{aij}u_iu_j+\frac{1}{\lambda_2^2}Q_{bij}B_iB_j+2\frac{1}{\lambda_1\lambda_2}(\mathbf{e}_a\cdot\mathbf{u})(\mathbf{e}_b\cdot\mathbf{B})\right]. \tag{3}$$

In (3), we have defined $\lambda_1\equiv1-(|p_0|+2|p_1|-p_0-p_1)/3$, $\lambda_2\equiv[q_0+2q_1+r_0+r_1]/3$. In addition, $d=n/36$ and $Q_{aij}\equiv(\mathbf{e}_a)_i(\mathbf{e}_a)_j-\delta_{ij}/2$.

The time evolution of the macroscopic fields is now found explicitly. The density is governed by a continuity equation $\partial n/\partial t+\nabla\cdot n\mathbf{u}=0$. The equation for momentum transport becomes $\partial n\mathbf{u}/\partial t+\nabla\cdot\mathbf{\Pi}=0$, where the momentum flux tensor $\mathbf{\Pi}\equiv\mathbf{\Pi}^{(0)}+\mathbf{\Pi}^{(1)}$, with $\mathbf{\Pi}^{(0)}=\sum_{ab}\mathbf{v}_{ab}\mathbf{v}_{ab}f_{ab}^{\rm eq}$ and $\mathbf{\Pi}^{(1)}=(1-\tau)\sum_{ab}\mathbf{v}_{ab}\mathbf{v}_{ab}[\partial f_{ab}^{\rm eq}/\partial t+\mathbf{v}_{ab}\cdot\nabla f_{ab}^{\rm eq}]$. Similarly, the magnetic-field transport equation is found to be $\partial n\mathbf{B}/\partial t+\nabla\cdot\mathbf{\Lambda}=0$, with $\mathbf{\Lambda}\equiv\mathbf{\Lambda}^{(0)}+\mathbf{\Lambda}^{(1)}$, with $\Lambda^{(0)}=\sum_{ab}(R_{ab}\mathbf{e}_a+Q_{ab}\mathbf{e}_b)\mathbf{v}_{ab}f_{ab}^{\rm eq}$ and

$$\mathbf{\Lambda}^{(1)}=(1-\tau)\sum_{ab}(R_{ab}\mathbf{e}_a+Q_{ab}\mathbf{e}_b)\mathbf{v}_{ab}[\partial f_{ab}^{\rm eq}/\partial t+\mathbf{v}_{ab}\cdot\nabla f_{ab}^{\rm eq}]\,.$$

These transport equations are easily further reduced to the form of the MHD equations by simplification of the flux tensors. All of the terms in the ideal MHD equations emerge from the flux tensors $\mathbf{\Pi}^{(0)}$ and $\Lambda^{(0)}$. In the limit of low speed and low magnetic field strength, the incompressible 2D MHD equations are thus obtained. An important difference between the CA model and this LBE model is that in the CA model a factor $G(n)\neq1$ appears in the final equations, representing non-Galilean invariance of the model, whereas here $G(n)\equiv1$ and Galilean invariance is restored.

The viscosities and resistivities in the LBE model are evaluated from the contributions of $\mathbf{\Pi}^{(1)}$ and $\mathbf{\Lambda}^{(1)}$ in the Chapman-Enskog expansion. Here the transport coefficients are more easily determined than in the CA model, by virtue of the simplified single-time (τ) relaxation approximation we have used for the collision integral. The exact results are

$$\nu=\frac{\tau-1}{12\lambda_1}[\tilde{p}_0^3+2\tilde{p}_1^3+3p_0\tilde{p}_0(\tilde{p}_0+p_0)+3p_1\tilde{p}_1(\tilde{p}_1+p_1)+p_0^3+p_1^3]+\frac{1}{24\lambda_1}[\tilde{p}_0|p_0|+\tilde{p}_0^2+2\tilde{p}_1^2+5|p_1|\tilde{p}_1+p_0+p_1]$$

and

$$\mu=\frac{\tau-1}{12\lambda_2}[r_1(\tilde{p}_1^2-p_1^2)+q_0(p_0^2+\tilde{p}_0^2)-2r_1p_1\tilde{p}_1+5q_1\tilde{p}_1^2+2q_0p_0\tilde{p}_0+2q_1p_1(\tilde{p}_1+p_1)]+\frac{1}{24\lambda_2}[q_0+q_1(5-3|p_1|)+r_1]\,,$$

where $\tilde{p}_0=1-|p_0|$ and $\tilde{p}_1=1-|p_1|$. For a given $\mathbf{P}$, $\mathbf{Q}$, and $\mathbf{R}$, we can vary τ to make ν and μ as small as possible, which will allow us to use the current model to simulate the high-Reynolds-number MHD flows. This completes the outline of the MHD LBE model.

Several numerical tests of the MHD LBE model have been carried out, using vectorized Cray YMP and parallel CM-2 implementations. The computational speed of the present model for the following problems is at least 2 times faster than the spectral code. For all tests, the streaming parameters were $p_0=-0.200$ and $p_1=0.1009$ (see Table I in

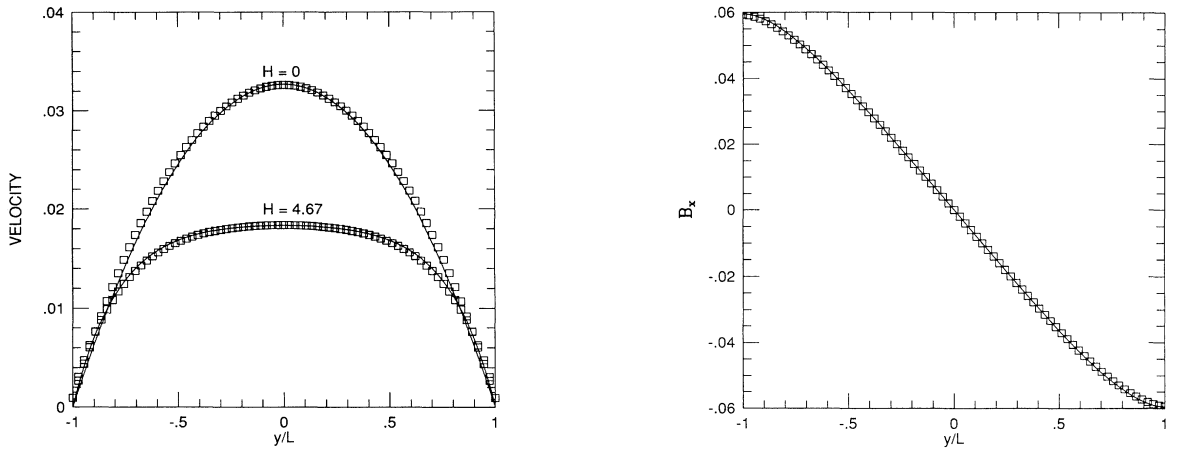

FIG. 1. Steady Hartmann flow profile, (left) $u_x(y)$ and (right) $B_x(y)$, from the MHD LBE model, for $H \approx 4.67$ and $H=0$ (no magnetic field). The numerical results (open squares) are compared with the corresponding analytical results (solid lines). The $H=0$ data are reduced in magnitude by a factor of 5 for convenience.

Ref. [5]). The relaxation time is $\tau=1.5$. A first set of tests (not shown here) has indicated that the model reproduces accurately the resonances expected in power spectra at frequencies and wave numbers that are solutions of the sound and Alfvén wave dispersion relations of linearized MHD. A second test problem is the case of steady Hartmann flow [11], a 2D forced channel flow with perfectly conducting boundaries. The channel boundaries are at $y=\pm L$, and $u_x(\pm L)=u_y(\pm L)=0$ and $\partial B_x(\pm L)/\partial y=0$ are enforced. For a forcing strength f, driving the streamwise velocity u_x, and an applied uniform, constant magnetic field across the channel of strength $B_y=B_0$, one has the steady solution $u_x(y)=U_0[1-\cosh(Hy/L)/\cosh H]$ and

$$B_x(y)=-B_0U_0\mu^{-1}[y-H^{-1}L\sinh(Hy/L)/\cosh H],$$

where the dimensionless Hartmann number $H\equiv B_0L/\sqrt{\mu\nu}$, and $U_0=fL^2/H^2n\nu$. Figure 1 shows the steady solution obtained using the MHD LBE scheme with a simulation size of 150×75 cells (channel width is 75 cells), for the cases $H=0$ (no magnetic field) and a second magnetized case, where $H\approx4.67$. The transport coefficients were evaluated using separate numerical experiments [12] (not shown) involving free Kolmogorov decay flows to be $\nu=0.236$ and $\mu=0.246$. These values agree with the theoretical expressions given above to at least three significant figures. It can be seen that the computed solution reverts to the parabolic channel flow profile for $H=0$, while the $H=4.67$ case also agrees extremely well with the inferred analytical solution.

As a third and final test discussed here we perform a simulation of the spatially periodic 2D incompressible

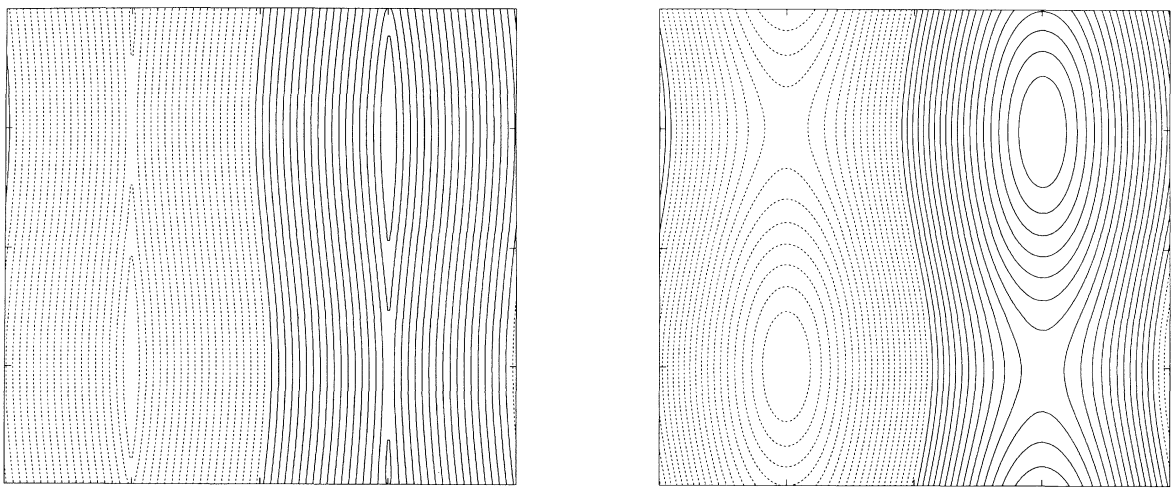

FIG. 2. Magnetic field line plots (contours of magnetic potential) for an early time (left) and a later time (right), $t\approx5.5$ MHD characteristic times, in a 256×256 cell MHD LBE simulation of the plane periodic sheet pinch. Magnetic reconnection, giving rise to growth of large magnetic islands, is evident.

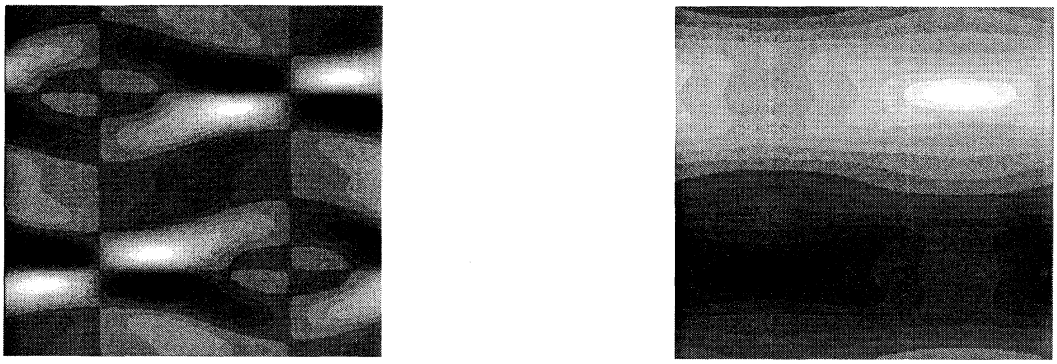

FIG. 3. Left: contours of vorticity at time $t \approx 5.5$, showing a quadrupolelike pattern of vorticity generation near magnetic X points. Right: shading plots of electric current density, also at $t \approx 5.5$. The LBE MHD model evidently captures both nonlinear and fine-scale aspects of the MHD solutions.

sheet pinch configuration [13], which is known to exhibit a pattern of complex and nonlinear behavior that falls generally under the description of magnetic reconnection. In Fig. 2, contour plots of magnetic field lines are shown, at a very early time, and again after several characteristic MHD times (1500 lattice-gas times at a characteristic magnetic field strength of 0.15) have elapsed. The well-known [13] phenomenon of magnetic island growth is evident. Magnetic reconnection is also typified by the appearance of organized small-spatial-scale structures that appear in the vicinity of the magnetic "X points" at the boundaries of the growing islands. These structures, which are somewhat coherent in time, can be described as a filamentation of electric current density at the X point, accompanied by a quadrupole pattern of vorticity centered around the X point. Figure 3 shows that these structures indeed are uncovered in the LBE dynamics, and have configurations that are quite similar to the analogous coherent structures found in many simulations, including high-resolution Fourier-spectral-method computations [13].

The MHD LBE model introduced in the present paper is easily implemented for a number of interesting and even complex MHD boundary conditions [12]. As described here, the LBE model avoids the CA difficulties with Galilean noninvariance, and with the single-time relaxation collision model, the viscosity and resistivity are independent of density. An additional advantage, not discussed above [11,14], is that the equation of state can be readily constrained to be, for example, exactly isothermal, again avoiding a problem with velocity-dependent pressure that plagues many CA implementations [15]. The first numerical tests of the MHD LBE model indicate clearly that the method captures the basic physics of MHD, in both qualitative and quantitative terms. Because of the simplicity and parallel nature of its coding and the capability to handle complex boundary conditions and shapes, we suspect that this model may provide a new approach to model numerically the dynamics of a variety of MHD systems, ranging from laboratory plasma fusion devices to space and astrophysical plasma flows. The potential of the model is greatly enhanced by its straightforward extension to 3D, and the soon-to-be-widespread availability of massively parallel computational facilities.

This research has been supported by NASA IRP Grant No. NAGW-1648, and by the U.S. DOE through Grant No. DE-FG02-85ER-53194 at Dartmouth and through LANL. Some of the computations were supported by the NSF SDSC, by the NASA CFCS, and by the ACL at Los Alamos.

[a]Present address: Center for Nonlinear Studies, Los Alamos National Laboratory, Los Alamos, NM 87545.
[b]Present address: Department of Physics and Astronomy, Dartmouth College, Hanover, NH 03755.

[1] U. Frisch, B. Hasslacher, and Y. Pomeau, Phys. Rev. Lett. **56**, 1505 (1986).
[2] U. Frisch, D. d'Humières, B. Hasslacher, P. Lallemand, Y. Pomeau, and J.-P. Rivet, Complex Syst. **1**, 649 (1987).
[3] S. Wolfram, J. Stat. Phys. **45**, 471 (1986).
[4] D. Montgomery and G. Doolen, Phys. Lett. A **120**, 229 (1987).
[5] H. Chen and W. H. Matthaeus, Phys. Rev. Lett. **58**, 1845 (1987); Phys. Fluids **31**, 1439 (1988).
[6] *Lattice Gas Methods for PDEs*, edited by G. Doolen (Addison-Wesley, New York, 1989).
[7] G. McNamara and G. Zanetti, Phys. Rev. Lett. **61**, 2332 (1988).
[8] F. Higuera and J. Jimenez, Europhys. Lett. **9**, 663 (1989).
[9] S. Succi, M. Vergassola, and R. Benzi, Phys. Rev. A **43**, 4521 (1991).
[10] K. Wang, *Statistical Mechanics* (Wiley, New York, 1963).
[11] J. A. Shercliff, *A Textbook of Magnetohydrodynamics* (Pergamon, New York, 1965), Sec. 6.5.
[12] W. Matthaeus, S. Chen, H. Chen, and D. Martínez (to be published).
[13] W. Matthaeus and S. Lamkin, Phys. Fluids **29**, 2513 (1986); W. Matthaeus and D. Montgomery, J. Plasma Phys. **25**, 11 (1981).
[14] H. Chen, S. Chen, and W. Matthaeus (to be published).
[15] J. Dahlburg, D. Montgomery, and G. Doolen, Phys. Rev. A **36**, 2471 (1987).

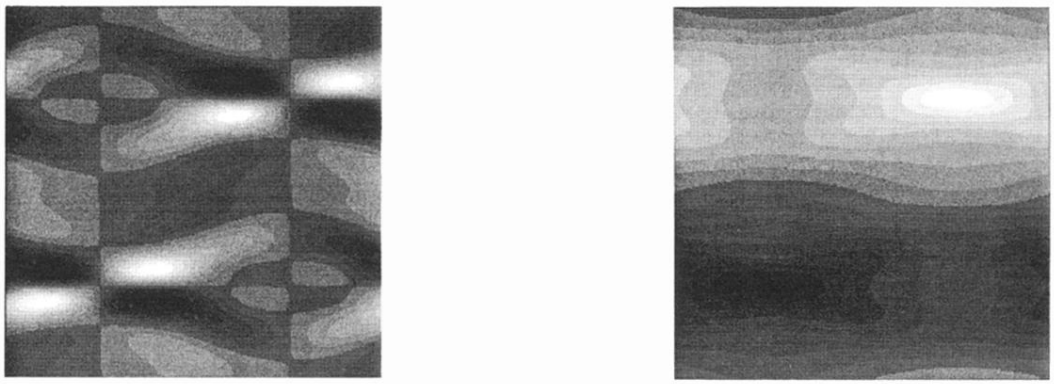

FIG. 3. Left: contours of vorticity at time $t \approx 5.5$, showing a quadrupolelike pattern of vorticity generation near magnetic X points. Right: shading plots of electric current density, also at $t \approx 5.5$. The LBE MHD model evidently captures both nonlinear and fine-scale aspects of the MHD solutions.